

1 **Comparison of six algorithms to determine the soil apparent thermal**
2 **diffusivity at a site in the Loess Plateau of China**

3
4 Linlin Wang¹, Robert Horton², Zhiqiu Gao¹

- 5
6 1. *State Key Laboratory of Atmospheric Boundary Layer Physics and Atmospheric Chemistry,*
7 *Institute of Atmospheric Physics, CAS, Beijing, China*
8 2. *Department of Agronomy, Iowa State University, Ames, Iowa, USA*

9
10 **Abstract**

11 Soil apparent thermal diffusivity is a crucial physical parameter that affects soil temperature.
12 Six prevalent algorithms to calculate soil apparent thermal diffusivity are inter-compared by using
13 soil temperature data collected at the depths of 0.05 m and 0.10 m at a bare site in the China
14 Loess Plateau from DOY 201 through DOY 207 in 2005. Five of the six algorithms (i.e.,
15 Amplitude, Phase, Arctangent, Logarithm, and Harmonic or HM algorithms) are developed from
16 the traditional one-dimensional heat conduction equation. The other algorithm is based on the
17 one-dimensional heat conduction-convection equation which considers the vertical heterogeneity
18 of thermal diffusivity in soil and couples thermal conduction and convection processes
19 (hereinafter referred to as the Conduction-convection algorithm). To assess these six algorithms,
20 we (1) calculate the soil apparent thermal diffusivities by using each of the algorithms, (2) use the
21 soil apparent thermal diffusivities to predict soil temperature at the 0.10 m depth, and (3) compare
22 the estimated soil temperature against direct measurements. Results show that (1) HM algorithm
23 gives the most reliable estimates among the traditional five algorithms; and (2) generally, the
24 Conduction-convection algorithm provides the second best estimates. Among all of the algorithms,
25 the HM algorithm has the best description of the upper boundary temperature with time, but it
26 only includes conduction heat transfer in the soil. Compared to the HM algorithm, the
27 Conduction-convection algorithm has a less accurate description of the upper boundary
28 temperature, but by accounting for the vertical gradient of soil diffusivity and the water flux
29 density it includes more physics in the soil heat transfer process. The Conduction-convection
30 algorithm has potential application within land surface models, but future effort should be made
31 to combine the HM and Conduction-convection algorithms in order to make use of the advantages

1 of each.

2

3

4

5 1. Introduction

6 Soil temperature plays an important role in land surface processes, and it is critical in energy
7 balance applications such as land surface modeling, numerical weather forecasting, and climate
8 prediction (Holmes et al., 2008). It is especially true for the soil surface. Accurate prediction of
9 soil surface temperature requires a realistic understanding of the soil thermal properties, i.e.,
10 volumetric heat capacity (C_g , $\text{J m}^{-3} \text{K}^{-1}$), thermal conductivity (λ , $\text{W m}^{-1} \text{K}^{-1}$), and thermal
11 diffusivity ($k = \lambda / C_g$, $\text{m}^2 \text{s}^{-1}$). The volumetric heat capacity C_g can be estimated as follows (De
12 Vries, 1963),

$$13 \quad C_g = (1 - \theta_s)C_s + \theta C_w, \quad (1)$$

14 where θ is the volumetric water content, θ_s is the saturated value of θ , and C_s and C_w are
15 the volumetric heat capacities of dry soil and water respectively. If C_g is known, only thermal
16 conductivity, λ , or thermal diffusivity, k , must be determined to characterize the thermal
17 properties of a soil (Passerat et al., 1996). k is of primary importance in determining soil
18 temperature propagation (Zhang and Osterkamp, 1995). Thermal diffusivity is based solely upon
19 conduction heat transfer. However, in soils, both conduction and convection heat transfer occur
20 simultaneously to impact soil temperature change. Often a single parameter conduction-alone
21 model is used to describe soil temperature changes. Since conduction and convection must be
22 accounted for by a single parameter, the parameter must be broader than conduction alone. The
23 parameter, often referred to as the soil thermal diffusivity, is more precisely the soil apparent
24 thermal diffusivity, because it accounts for conduction and convection heat transfer processes that

1 affect soil temperature change. Several algorithms have been proposed to estimate soil apparent
2 thermal diffusivity. Most of the algorithms are based on solutions of the one-dimensional
3 conduction heat transfer equation. Lettau (1971) calculated the apparent thermal diffusivity as a
4 function of depth below the soil surface. In order to utilize this algorithm, measurements of soil
5 temperature with time are required at the soil surface and at several subsurface depths. However,
6 the lack of soil temperature data at several subsurface depths often limits the utility of this
7 algorithm (Horton et al., 1983). Assuming that the apparent thermal diffusivity is independent of
8 depth, and considering that temperature at the upper boundary is well described by a sinusoidal
9 function, the analytical solution of the one-dimensional heat conduction equation can be used to
10 estimate apparent k . Based on this solution, the apparent thermal diffusivity can be estimated by
11 the Amplitude algorithm and Phase algorithm. Errors due to the assumption of single sinusoidal
12 temperature wave at the soil surface can be reduced by using a Fourier series to accurately
13 describe the diurnal variation in surface soil temperature (Van Wijk, 1963). In this way, the
14 apparent thermal diffusivity is estimated by the Arctangent algorithm (Nerpin and Chudnovskii,
15 1967) with two harmonics. It was shown by Seemann (1979) that, in analogy to the Arctangent
16 algorithm, the apparent thermal diffusivity can also be calculated by the Logarithmic algorithm.
17 These two algorithms are analogous to the Amplitude algorithm and Phase algorithm but take
18 advantage of greater number of temperature observations to approximate a potentially
19 nonsinusoidal behavior (Horton et al., 1983). However, a two-harmonic function cannot describe
20 the surface temperature very well, and a series of harmonics for the upper boundary offers
21 advantages. Based on this boundary, the solution of the one-dimensional heat conduction equation
22 is developed from the assumption of a sinusoidal function. According to the solution, the apparent

1 thermal diffusivity can be selected to minimize the sum of squared differences between the
2 calculated and measured soil temperature values (Horton et al., 1983). And it can also be
3 estimated from an iteration process by fitting the amplitude and phase of soil temperature at one
4 depth (Heusinkveld et al., 2004). All algorithms mentioned above are based on solutions of the
5 one-dimensional conduction heat equation and constant diffusivity, and thus apply to uniform
6 soils only. In fact, soil heat transfer is caused by a combination of conduction and intra-porous
7 liquid and vapor convection (Passerat et al., 1996). Verhoef et al.(1996) described the course of
8 topsoil thermal conductivity, diffusivity, and heat capacity during two measurement campaigns,
9 conducted in semi-arid areas—the EFEDA-I experiment and HAPEX-Sahel. In the derivation of
10 apparent thermal diffusivity five methods (the Amplitude, Phase, Arctangent, Logarithmic and
11 Harmonic equation) were compared. Gao et al. (2003) pointed out that soil temperature changes
12 in response to both conduction and convection processes, where convection was understood as
13 ‘vertical heat transfer caused by the vertical movement of liquid water in the soil’. They solved
14 analytically the equation for one-dimensional conduction-convection, and derived a simple
15 algorithm to accurately estimate soil thermal diffusivity.

16 Few efforts have been made to quantitatively test the various k algorithms by using an
17 identical soil temperature data set. The land-air interaction over the Loess Plateau located in
18 mid-western China affects the weather and climate in northwest China. A realistic description of
19 soil temperature helps better understanding the land-air interaction over the Loess Plateau
20 however few attempts have been made to determine the Loess Plateau soil thermal parameters for
21 soil temperature algorithms. The measurements of soil temperature and soil water content during
22 the LOess Plateau land surface process field EXperiment (LOPEX) in 2005 provided us an
23 opportunity to evaluate the k algorithms for use on Loess Plateau soil. In order to improve the
24 accurate knowledge of the soil apparent thermal diffusivity in this area, the objective of this paper
25 is to compare six algorithms for determination of the soil apparent thermal diffusivity by using the

1 direct measurements of soil temperature restricted to the upper 0.1 m of soil.

2

3 2. Theoretical considerations

4 Previous algorithms to calculate soil apparent thermal diffusivity k are listed in Table 1.

5 2.1. Classical thermal conduction equation for soil temperature

6 Conduction heat transfer in a one-dimensional isotropic medium is described by

$$7 \quad C_g \frac{\partial T}{\partial t} = \frac{\partial}{\partial z} \left(\lambda \frac{\partial T}{\partial z} \right), \quad (2)$$

8 where T is the soil temperature (K), t the time (s), z the depth (m), C_g the volumetric heat
9 capacity ($\text{J m}^{-3} \text{K}^{-1}$), and λ the thermal conductivity ($\text{W m}^{-1} \text{K}^{-1}$). Assuming that a soil is
10 vertically homogeneous, in this case that C_g and λ are independent of depth, provides

$$11 \quad \frac{\partial T}{\partial t} = k \frac{\partial^2 T}{\partial z^2}, \quad (3)$$

12 where k for soil is referred to as the apparent thermal diffusivity The following five algorithms
13 based on the solution of Eq. (3) have been used to estimate k .

14 2.1.1. Amplitude Algorithm

15 Given the surface boundary condition:

$$16 \quad T|_{z=0} = \bar{T} + A \sin(\omega t + \Phi), \quad (t \geq 0), \quad (4)$$

17 where \bar{T} is the mean soil surface temperature, A is the amplitude of the diurnal soil surface
18 temperature wave, and ω is the angular velocity of the Earth's rotation and $\omega = 2\pi / P$ (rad s^{-1})
19 with P representing the period of the diurnal cycle. The soil temperature (T) at a depth z can
20 be calculated via

$$21 \quad T(z, t) = \bar{T} + A \exp(-z/d) \sin(\omega t - z/d + \Phi), \quad (5)$$

22 here $d = \sqrt{2k/\omega}$ is the damping depth of the diurnal temperature wave.

23 Soil temperature measured at two different depths (z_1 and z_2) are often assumed to be
24 approximated by a sinusoidal function when estimating k . The sinusoidal functions are given by

$$25 \quad T|_{z=z_1} = \bar{T}_1 + A_1 \sin(\omega t + \Phi_1), \quad (6)$$

1 and $T|_{z=z_2} = \bar{T}_2 + A_2 \sin(\omega t + \Phi_2)$, (7)

2 where A_1 (A_2), Φ_1 (Φ_2) and \bar{T}_1 (\bar{T}_2) are the amplitude, phase and mean soil temperature at
3 the depth z_1 (z_2). \bar{T}_1 (\bar{T}_2) is the arithmetical average of the daytime maximum soil temperature
4 and the nighttime minimum soil temperature; and A_1 (A_2) is half of the difference between the
5 daytime maximum value and the nighttime minimum value for soil depth of z_1 (z_2); and Φ_1
6 (Φ_2) is the initial phase of soil temperature at depth z_1 (z_2), obtained by using the best fit
7 algorithm (Horton et al., 1983). Then the apparent thermal diffusivity k is determined by the
8 Amplitude algorithm

9
$$k = \frac{\omega(z_1 - z_2)^2}{2 \ln(A_1/A_2)^2}$$
 (8)

10 *2.1.2. Phase Algorithm*

11 If the time interval between the measured occurrences of maximum soil temperature at the
12 depths of z_1 and z_2 is $\Delta t = t_2 - t_1$, the Phase algorithm stemming from Eq. (4) is (Horton et al.,
13 1983)

14
$$k = \frac{\omega(z_1 - z_2)^2}{2(\Phi_1 - \Phi_2)^2}$$
 (9)

15 *2.1.3. Arctangent Algorithm*

16 Soil surface temperature can be described by a Fourier series:

17
$$T = \bar{T} + \sum_{i=1}^n [a_i \sin(i\omega t) + b_i \cos(i\omega t)],$$
 (10)

18 where n is the number of harmonics, and a_i and b_i are the amplitudes. Setting $n = 2$, k
19 can be calculated by the Arctangent algorithm

20
$$k = \frac{\omega \Delta z^2}{2 \left\{ \arctan \left[\frac{(T_1 - T_3)(T_2' - T_4') - (T_2 - T_4)(T_1' - T_3')}{(T_1 - T_3)(T_1' - T_3') + (T_2 - T_4)(T_2' - T_4')} \right] \right\}^2},$$
 (11)

21 where temperatures T_j and T_j' are recorded each 6 h ($j = 1, 2, 3, \text{ and } 4$) at two different depths
22 z_1 and z_2 , respectively. The first reading is taken at 02:00 (Local time, hereinafter, referred to as

1 LT), then 08:00 (LT), 14:00 (LT), 20:00 (LT).

2 2.1.4. Logarithmic Algorithm

3 Using the same assumption of the Arctangent algorithm, k is expressed by

$$4 \quad k = \left\{ \frac{0.0121\Delta z}{\ln \left[\frac{(T_1 - T_3)^2 + (T_2 - T_4)^2}{(T_1' - T_3')^2 + (T_2' - T_4')^2} \right]} \right\}^2. \quad (12)$$

5 2.1.5. Harmonic Algorithm

6 Eq. (10) can also be changed into another form as

$$7 \quad T = \bar{T} + \sum_{i=1}^n C_i \sin(i\omega t + \Phi_i), \quad (13)$$

8 where C_i is the amplitude of the harmonic i :

$$9 \quad C_i = \sqrt{a_i^2 + b_i^2}, \quad (14)$$

10 and Φ_i is the phase of the harmonic i :

$$11 \quad \Phi_i = \arctan(a_i / b_i). \quad (15)$$

12 Given the following boundary condition:

$$13 \quad T|_{z=0} = \bar{T} + \sum_{i=1}^n C_{0i} \sin(i\omega t + \Phi_{0i}), \quad (t \geq 0), \quad (16)$$

14 the solution of Eq. (3) is

$$15 \quad T(z, t) = \bar{T} + \sum_{i=1}^n C_{0i} \exp(-z / d_i) \sin(i\omega t + \Phi_{0i} - z / d_i), \quad (17)$$

16 where C_{0i} and Φ_{0i} are the amplitude and phase of the harmonic i for the upper depth,

17 respectively, and $d_i = \sqrt{2k / (i\omega)}$ corresponds to the depth at which the signal is propagated

18 during a period P / i . Based on Eq. (17), the apparent thermal diffusivity k can be determined

19 by the Least Squares Algorithm (Horton et al., 1983). On the other hand, C_{1i} (C_{2i}) and Φ_{1i}

20 (Φ_{2i}) at the depth of z_1 (z_2) can be obtained by the approximation of the observed data at these

21 two depths with the harmonic curve fit. In addition, according to Eq. (17), the amplitude C_{2i} and

22 initial phase Φ_{2i} at the depth of z_2 can be predicted from

1
$$C_{2i} = C_{1i} \exp(-z/d_i), \quad (18)$$

2 and
$$\Phi_{2i} = \Phi_{1i} - z/d_i. \quad (19)$$

3 After an initial guess of k , the predicted results of amplitude and initial phase are compared with
 4 the fitted ones, and the parameter is adjusted depending on the differences in amplitude and initial
 5 phase (Heusinkveld et al., 2004).

6

7 *2.2. Soil temperature rate equation with vertical heterogeneity of soil thermal diffusivity coupled*
 8 *with thermal conduction and heat transfer by water flux*

9 Eq. (3) assumes that k is independent of depth, however, k can vary (increase or decrease)
 10 from the surface downward in the shallow surface layer of most soils. Eq. (2) can therefore be
 11 improved as follows (Gao et al., 2008):

12
$$\frac{\partial T}{\partial t} = \frac{1}{C_g} \frac{\partial}{\partial z} \left(\lambda \frac{\partial T}{\partial z} \right) = \frac{\lambda}{C_g} \frac{\partial^2 T}{\partial z^2} + \frac{1}{C_g} \frac{\partial \lambda}{\partial z} \frac{\partial T}{\partial z} \approx k \frac{\partial^2 T}{\partial z^2} + \frac{\partial k}{\partial z} \frac{\partial T}{\partial z}. \quad (20)$$

13 Neglecting the vertical heterogeneity of k , Gao et al. (2003) incorporated thermal conduction
 14 and convection together as follows:

15
$$\frac{\partial T}{\partial t} = k \frac{\partial^2 T}{\partial z^2} - \frac{C_w}{C_s} w \theta \frac{\partial T}{\partial z}. \quad (21)$$

16 where w is the liquid flow rate (positive downward) and θ is the volumetric water content of
 17 the soil. C_w is the heat capacity of water. Assuming these three parameters are also independent

18 of z for a thin soil layer in present work, $-\frac{C_w}{C_s} w \theta$ was defined as water flux by Gao et al.

19 (2003). Based on Eqs. (19) and (21), Gao et al. (2008) presented the following equation

20
$$\frac{\partial T}{\partial t} = k \frac{\partial^2 T}{\partial z^2} + W \frac{\partial T}{\partial z}, \quad (22)$$

21 where $W = \frac{\partial k}{\partial z} - \frac{C_w}{C_s} w \theta$ consisted of the vertical gradient of soil diffusivity ($\frac{\partial k}{\partial z}$) and the water

22 flux density ($-\frac{C_w}{C_s} w \theta$).

1 With the boundary condition Eq. (7), the expression of the soil temperature at the depth z_1 is

$$2 \quad T(z_1, t) = \bar{T}_1 + A_2 \exp[-\alpha(z_1 - z_2)M] \sin[\omega t + \Phi_2 - \alpha(z_1 - z_2)N], \quad (23)$$

3 where $M = \frac{\alpha}{\omega} \left\{ W + \frac{1}{\sqrt{2}} \left[W^2 + \left(W^4 + \frac{4\omega^4}{\alpha^4} \right)^{1/2} \right]^{1/2} \right\}$ and $N = \sqrt{2} \left(\frac{\omega}{\alpha} \right) \left[W^2 + \left(W^4 + \frac{4\omega^4}{\alpha^4} \right)^{1/2} \right]^{-1/2}$.

4 They also gave the expression of k and W

$$5 \quad k = -\frac{(z_1 - z_2)^2 \omega \ln(A_1 / A_2)}{(\Phi_1 - \Phi_2) \left[(\Phi_1 - \Phi_2)^2 + \ln^2(A_1 / A_2) \right]}, \quad (24)$$

$$6 \quad W = \frac{\omega(z_1 - z_2)}{\Phi_1 - \Phi_2} \left[\frac{2 \ln^2(A_1 / A_2)}{(\Phi_1 - \Phi_2)^2 + \ln^2(A_1 / A_2)} - 1 \right]. \quad (25)$$

7 We call it as Conduction-convection algorithm in this paper. Applying $W = 0$ to Eq. (25) results
 8 in $\Phi_2 - \Phi_1 = -\ln(A_2 / A_1)$ or $-\ln(A_2 / A_1) = \Phi_2 - \Phi_1$, then Eq. (24) reduces to be Eq. (8) or Eq.
 9 (9).

10

11 **3. Field Experiments**

12 The experiment was conducted on soil in the China Loess Plateau during an intensive
 13 observation period from DOY 197 through 241 in LOPEX in 2005. The soil measurements were
 14 collected at a bare soil site located at 106.42°E, 35.35°N at an altitude of 1592 m in Pingliang
 15 county of Gansu Province in western China.

16 The ground surface of this site was bare, flat and homogeneous. The soil at the site was
 17 predominantly medium loam with a high proportion of silt. The site is located within a semiarid
 18 climate zone. The maximum air temperature was 307 K and the lowest was 249 K, the annual air
 19 temperature and precipitation were 279K and 510 mm with 2425 hours of sunshine, and 170
 20 frost-free days per year all averaged over the last 50 years (Gao et al., 2008). The bulk density
 21 was 1250 kg m⁻³, and soil solid heat capacity was 1.40×10⁶ J m⁻³ K⁻¹.

22 Soil temperature was measured with four TCAV averaging soil thermocouple probes
 23 (Campbell Scientific Inc., U.S.A.) at 0.05 and 0.10 m depths. The volumetric water content of the
 24 soil was measured at 0.05 and 0.10 m depths by two soil moisture reflectometers (CS615,
 25 Campbell Scientific Inc. USA). All of the sensor outputs were recorded and averaged over 10 min

1 intervals.

2

3 **4. Results**

4 The data used in this paper were collected in a 7-day period from (DOYs 201 through 207 (i.e.,
5 20 through 26 July), 2005. The soil temperature measured at 0.05 and 0.10 m depths changed
6 diurnally during DOYs 203-207, as shown in Figure 1a. The amplitudes of the soil temperature
7 decreased and the phases shifted ahead when the soil depth increased. The soil temperature at
8 0.05 m changed in response to intermittent cloudiness during DOYs 202 and 203. The maximum
9 soil temperature reached 310.78 K on DOY 204, and the minimum soil temperature was 287.77 K
10 at 0.05 m depth on DOY 203. Figure 1a also shows that the soil vertical temperature gradient
11 reached 191.20 K m⁻¹ for the soil layer from 0.05 to 0.10 m depths at 14:45 (LT) on DOY 204 at
12 this site.

13 The temporal variations in volumetric soil water content at 0.05 and 0.10 m depths during
14 the same period are shown in Figure 1b. Precipitation occurred from DOYs 199 to 201 with an
15 amount of 15.7 mm. Since then, owing to evaporation from the bare soil surface, the soil
16 volumetric water content was decreasing gradually at both depths from DOYs 202 through 207.
17 Gao et al. (2008) pointed out that under evaporation conditions there is a net upward flux of water
18 (liquid and vapor) that responds to the progressively drying surface condition. The net flux of
19 water causes an associated net convective heat flux. The soil physics implies that the heat transfer
20 should incorporate a vertical convective heat transfer component.

21 After using a 2-hour smoothing technique for soil temperature measured at the depth of 0.05
22 m, A_1 , A_2 , Φ_1 , Φ_2 , \bar{T}_1 , \bar{T}_2 , \bar{T} , C_i and Φ_i are obtained by using the approximation of
23 soil temperature collected at the depths of 0.05 m and 0.10 m for each day, respectively.
24 Smoothing reduces amplitudes, but we are concerned with A_1/A_2 . The reduction in both A_1 and A_2
25 does not influence A_1/A_2 much. The temporal variations of k are calculated by using the
26 Amplitude, Phase, Conduction-convection and HM algorithms (Horton et al., 1983, Heusinkveld
27 et al., 2004, Gao et al., 2008) for the soil layer from 0.05 m to 0.10 m. Temperatures at each depth
28 for the arbitrary times of 02:00 (LT), 08:00 (LT), 14:00 (LT), and 20:00 (LT) were used for

1 Arctangent algorithm and Logarithmic algorithm. Results are shown in Figure 2. The Amplitude,
2 Arctangent, Logarithmic and HM algorithms provided relatively low values of k during this
3 period. This is especially true for the Arctangent algorithm. The Phase algorithm and the
4 Conduction-convection algorithm provided k values approximately twice as large as the other
5 algorithms. The two HM algorithms provided similar values of k . The thermal diffusivity
6 estimated by the Logarithmic algorithm changed from day to day in the drying period. The
7 maximum, minimum and mean values of k calculated by these six algorithms are listed in Table
8 2. The smallest value of k is $0.6 \times 10^{-7} \text{ m}^2 \text{ s}^{-1}$, and it is obtained from the Arctangent algorithm
9 on DOY 202. The maximum value is $5.47 \times 10^{-7} \text{ m}^2 \text{ s}^{-1}$, and it is obtained from the Phase
10 algorithm on DOY 207. The maximum, minimum and mean values of k calculated by the Phase
11 algorithm and by the Conduction-convection algorithm are larger than the values derived by the
12 other algorithms. The two HM algorithms and the Amplitude algorithm provide similar estimates
13 of the mean values of k .

14

15 **5. Discussion**

16 The variations of the apparent thermal diffusivity k obtained by the six algorithms with the
17 volumetric soil water content θ for the 0.05 m to 0.10 m layer are shown in Figure 3. Estimates
18 of k from five of the six algorithms change in a narrow range with θ during this drying period
19 ($\theta < 25\%$). The exception is the Logarithmic algorithm. The values of k from the Phase
20 algorithm and the Conduction-convection algorithm have similar trends with θ . The variations
21 of k shown by the other four algorithms show a similar trend with θ . These results make sense
22 because values of k from the Phase and the Conduction-convection algorithms mainly depend
23 on $\Phi_1 - \Phi_2$, while estimates of k with the other algorithms mainly depend on the amplitude.
24 All of the algorithms indicate that the largest value of k does not occur at the largest soil water
25 content. Gao et al. (2008) showed that k does not monotonically increase with increasing θ . It
26 tends to increase as dry soil begins to wet, but it approaches a constant value or even decreases as
27 the soil continues to wet.

28 In the Conduction-convection algorithm, another parameter W is needed and is calculated

1 with Eq. (25) (see values in Table 3).

2 The measured and modeled soil temperatures at the 0.10 m depth from DOY 201 through 207
3 are presented in Figure 4. It is obvious that the fitted temperature by using Arctangent,
4 Logarithmic and the two HM algorithms gave poor approximation in the early morning of DOY
5 203 because the assumption of repeating surface periodic temperature is not valid between DOY
6 202 and 203. To better show the model outputs, we take DOY 204 as an example (see Figure 5).
7 Overall, The Phase algorithm reasonably estimated the soil temperature phases but overestimated
8 the amplitudes, and the amplitude algorithm reasonably estimated the soil temperature amplitudes
9 but overestimated the phase shift. In fact, as shown in Table 4, the values of $\ln(A_1/A_2)$ are larger
10 than $\Phi_1 - \Phi_2$ for the whole 7-day period. Using the Phase algorithm to estimate k implies
11 forcing $\ln(A_1/A_2)$ to be equal to $\Phi_1 - \Phi_2$, which overestimates the soil temperature amplitude
12 by about 0.74 K on average for DOYs 201 to 207. Similarly, using the Amplitude algorithm to
13 estimate k implies that $\Phi_1 - \Phi_2$ is equal to $\ln(A_1/A_2)$, which overestimates the soil
14 temperature phase shift by $\ln(A_1/A_2) - (\Phi_1 - \Phi_2) = 0.2397$ rad (55 minutes) on average for
15 DOYs 201 to 207.

16 The Logarithmic and Arctangent algorithms require four pairs of soil temperature
17 measurements. The modeled k values are very sensitive to the measurement time of four pairs
18 of soil temperatures, so we have to average the calculated values of k for different selections of
19 four pairs of soil temperatures for each day.

20 The two HM algorithms generated similar values of k . For most of the study days, the HM
21 algorithm gave realistic estimations of soil temperature at the depth of 0.10 m. However, as
22 mentioned above, it did not give a good estimation in the early morning of DOY 203 because of
23 the invalid assumption of the repeating periodic for soil temperature. Results obtained by two HM
24 algorithms indicate that fitting measurements of soil temperature by using the Least Squares
25 approach directly and simultaneously determining the amplitude and initial phase of the soil
26 temperature may provide realistic values of k . Comparison of the results obtained by the HM
27 algorithms, Phase algorithm, Amplitude algorithm, Logarithmic algorithm and Arctangent
28 algorithm shows that the HM algorithms gave the most accurate values of k . This conclusion

1 agrees with those by both Horton et al. (1983) and Verhoef et al. (1996).

2 The Conduction-convection algorithm provided realistic daytime soil temperature values.
3 However, it underestimated the soil temperature during the period from 18:00 (LT) to 08:00 (LT),
4 and a noteworthy difference between the measurements and the model output occurred around
5 00:00 (LT) for all days in this study. A similar underestimation was also encountered by Lin (1980)
6 and Gao et al. (2008). Our explanation is that the model always keeps W constant although the
7 actual W may decrease to zero or even become negative during the nighttime, and also the
8 model does not account for water phase changes that usually happen in shallow soil during the
9 nighttime.

10 Scatter plots of soil temperature modeled by using the six algorithms against the measured
11 soil temperature at the depth of 0.1 m are given in Figure 6. The results show that the HM
12 algorithms and Conduction-convection algorithm generated larger correlation coefficients (r),
13 than did the other algorithms. All of the regression lines had slopes of 1.

14 Statistical analyses are also used to examine the error of model output as follows,

$$15 \quad SEE = \sqrt{\frac{\sum_{i=1}^n (T_m - T)^2}{n - 2}}, \quad (26)$$

$$16 \quad NSEE = \sqrt{\frac{\sum_{i=1}^n (T_m - T)^2}{\sum_{i=1}^n T^2}}. \quad (27)$$

17 Where n is the total number of data points; SEE is the standard error of the estimate; and $NSEE$
18 is a normalized SEE which denotes an estimate of relative uncertainty. The statistical indices
19 SEE and $NSEE$ are presented in Table 5 for the modeled period. It is obvious that the HM
20 algorithm has the lowest values both of SEE and $NSEE$. The Conduction-convection algorithm
21 has the second lowest values of SEE and $NSEE$.

22 Another comparison of the accuracies of the six algorithms is shown in Figure 7 using the
23 empirical probability distribution functions (PDF) of difference between the modeled and
24 measured soil temperatures at the depth of 0.10 m. The differences between the modeled and
25 measured soil temperatures using the HM algorithm ranged between -1 K and 1 K, and most were
26 near zero. The Conduction-convection algorithm generated the second best results.

1

2 **6. Conclusions**

3 Six algorithms for calculating soil apparent thermal diffusivity are evaluated with shallow soil
4 measurements collected during LOPEX in 2005. The Phase algorithm and the Amplitude
5 algorithm overestimated the phase and overestimated the amplitude of the soil temperature,
6 respectively. Although the Arctangent algorithm and the Logarithmic algorithm only required four
7 measures of temperature spaced equally in time at two depths, the timing of the four measures of
8 temperature affected the values of soil apparent thermal diffusivity greatly. The HM algorithm
9 gave a reasonable result for most days. However, the assumption of repeating periodicity for soil
10 temperature is invalid on cloudy or rainy days. The algorithms mentioned above are based upon
11 the one-dimensional conduction equation. The Conduction-convection algorithm which is based
12 on the one-dimensional conduction-convection equation, provided satisfactory results for daytime
13 temperatures, but it systematically underestimated nighttime soil temperatures. Overall, the
14 Conduction-convection algorithm provided better results than all of the other algorithms except
15 for the HM algorithm. Future efforts should focus on combining the HM and the
16 Conduction-convection algorithms in order to develop an improved method that combines the
17 advantages of each algorithm. The new method should include multiple harmonics to describe
18 the upper boundary temperatures and include conduction and convection heat transfer processes.

19

20

21 **Acknowledgements**

22 This study was supported by MOST (2006CB403600, 2006CB400500), by CMA
23 (GYHY(QX)2007-6-5), and by the Centurial Program sponsored by the Chinese Academy
24 of Sciences. The work described in this publication was also supported by the European
25 Commission (Call FP7-ENV-2007-1 Grant nr. 212921) as part of the CEOP – AEGIS
26 project (<http://www.ceop-aegis.org/>) coordinated by the Université Louis Pasteur. This
27 study was partly supported by the Hatch Act and State of Iowa funds. The LOPEX05 field
28 campaign was supported by a grant from the Centurial Program sponsored by the Chinese

1 Academy of Sciences (2004406) and the field station foundation of the Chinese Academy
2 of Sciences. Equipment and logistical support was from the Pingliang Lightning and Hail
3 Storm Experiment Station of the Chinese Academy of Sciences. We are very grateful to Dr.
4 G. H. de Rooij and the anonymous reviewers for their careful reviews and valuable
5 comments, which led to substantial improvement of this manuscript.

6
7

8 **References**

- 9 Gao, Z, Fan, X. and Bian L. 2003. An analytical solution to one-dimensional thermal
10 conduction-convection in soil. *Soil Science*, 168, 99-107.
- 11 Gao, Z., D. H. Lenschow, R. Horton, M. Zhou, L. Wang, and J. Wen 2008, Comparison of Two
12 Soil Temperature Algorithms for a Bare Ground Site on the Loess Plateau in China, *J.*
13 *Geophys. Res.*, 113, doi:10.1029/2008JD010285.
- 14 Heusinkveld, B. G., A. F. G. Jacobs, A. A. M. Holtslag, and S. M. Berkowicz, 2004: Surface
15 energy balance closure in an arid region: role of soil heat flux, *Agricultural and Forest*
16 *Meteorology*, 122, 21-31.
- 17 Holmes, T. R. H., M. Owe, R. A. M. Jeu De, and H. Kooi, 2008: Estimating soil temperature
18 profile from a single depth observation: A simple empirical heat flow solution. *Water*
19 *Resources Research*, 44, W02412, doi:10.1029/2007WR005994.
- 20 Horton, R., P. J. Wierenga, and D. R. Nielsen, 1983: Evaluation of methods for determination
21 apparent thermal diffusivity of soil near the surface. *Soil Sci. Soc. Am. J.*, 47: 23-32
- 22 Lettau, B, 1971: Determination of thermal diffusion in the upper layers of a natural ground cover,

1 *Soil Science*, 112, 173-177

2 Lin, J. D., 1980: On the force-restore method for prediction of ground surface temperature, *J.*
3 *Geophys. Res.*, 85(C6), 3251-3254

4 Nerpin, S.V., and A.F. Chudnovskii, 1967: Physics of the soil, Israel Program for Scientific
5 Translations. Keter press, Jerusalem

6 Passerat de Silans, A. M. B., B. A. Monteny and J. P. Lhomme, 1996: Apparent soil thermal
7 diffusivity, a case study: HAPEX-Sahel experiment, *Agricultural and Forest Meteorology*,
8 81: 201-216

9 Seemann, J, 1979: Measurement technology. P. 40-45 In Seemann etal. (ed). Agrometeorology.
10 Springer-Verlag, Berlin

11 Zhang, T., Osterkamp, T.E., 1995: Considerations in determining thermal diffusivity from
12 temperature time series using finite difference methods. *Cold Region and Technology*, 23,
13 333-341

14 Van Wijk, W. R., De Vries, D. A., 1963: Periodic temperature variations in a homogeneous soil.
15 In: Van Wijk, W. R. (Ed.), *Physics of Plant Environment*. North-Holland Amsterdam, pp.
16 103-143

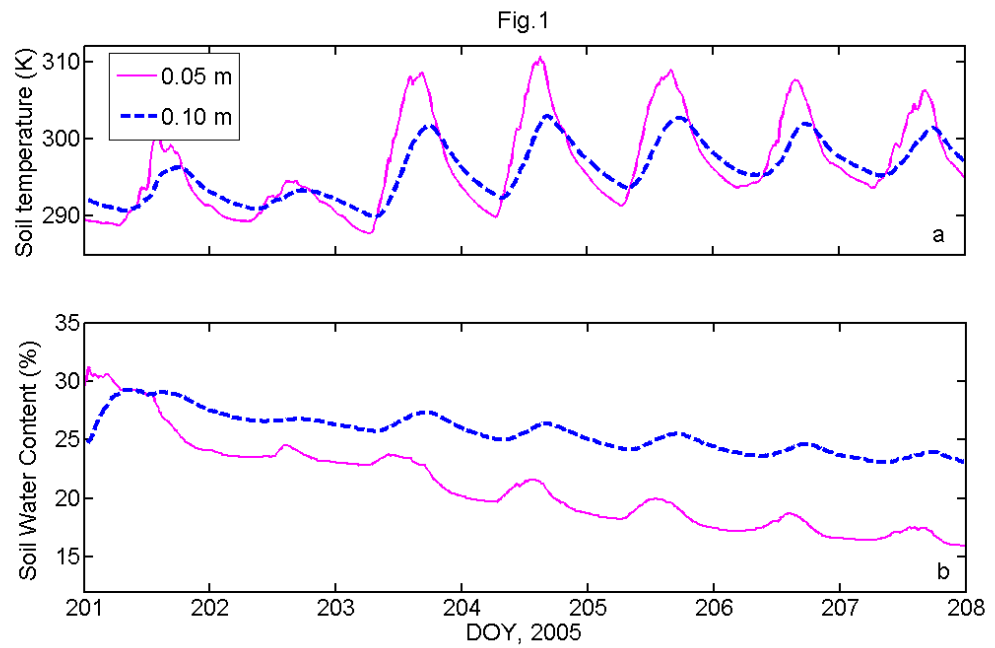
17 Verhoef A., Van den Hurk, B. J. J. M, Jacobs, and A. F.G. Heusinkveld, 1996: Thermal soil
18 properties for a vineyard (EFEDA-I) and a savanna (HAPEX-Sahel) site, *Agricultural*
19 *Forest Meteorology*, 78:1-18

20

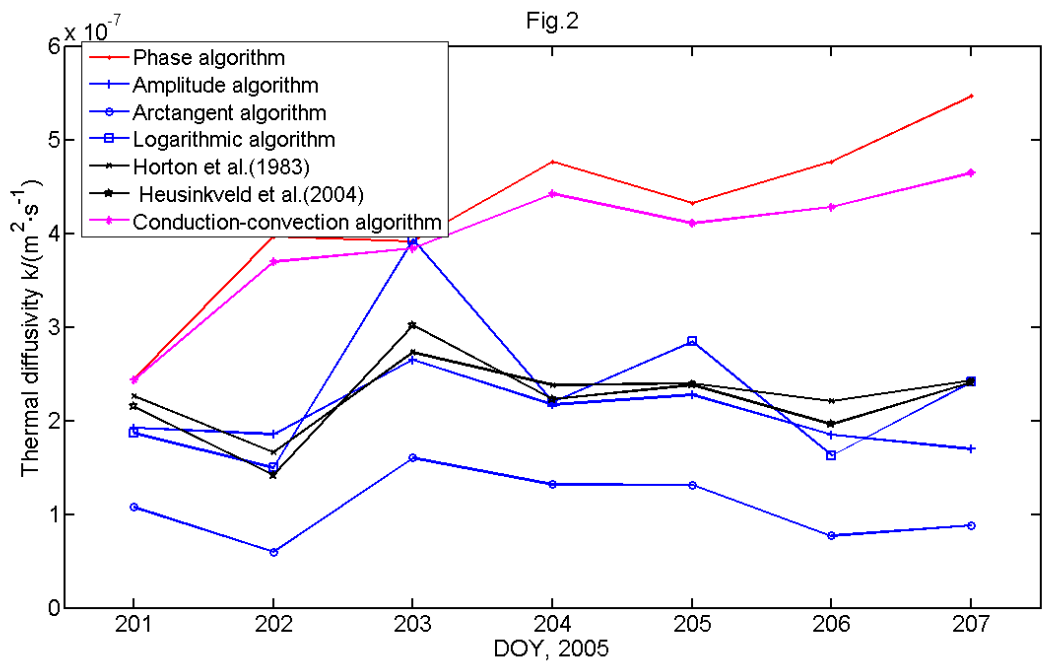
21

22 **Figures:**

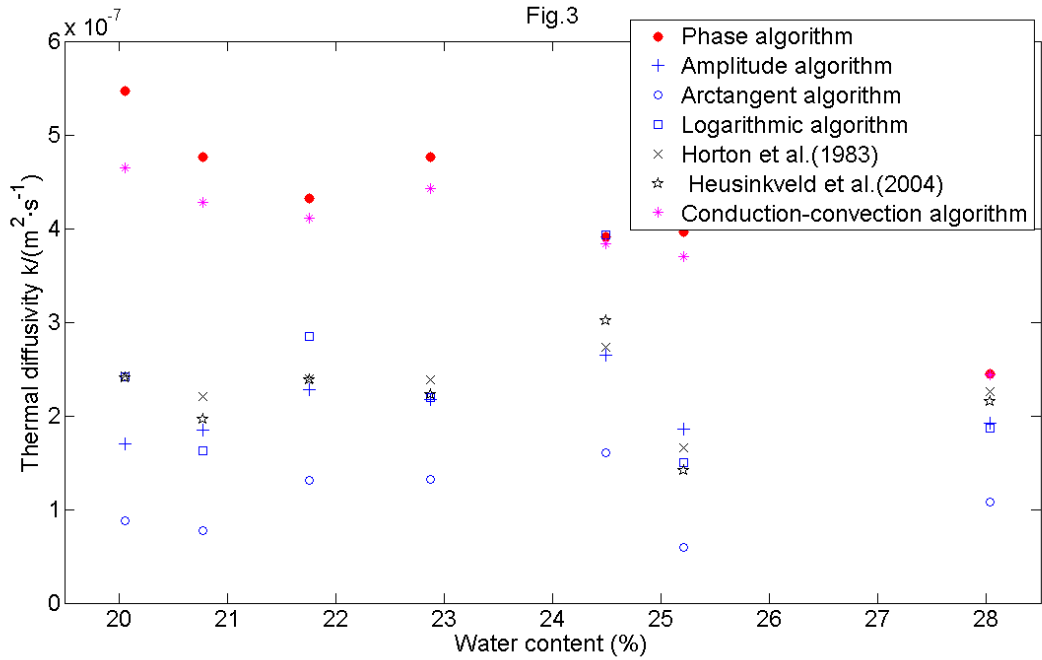
23



1
 2 Figure 1. Temporal variations of (a) soil temperature (K) and (b) soil water content (%) measured
 3 at depths of 0.05 m and 0.10 m at a bare soil site over the Loess Plateau from DOY 201 through
 4 DOY 207, 2005.

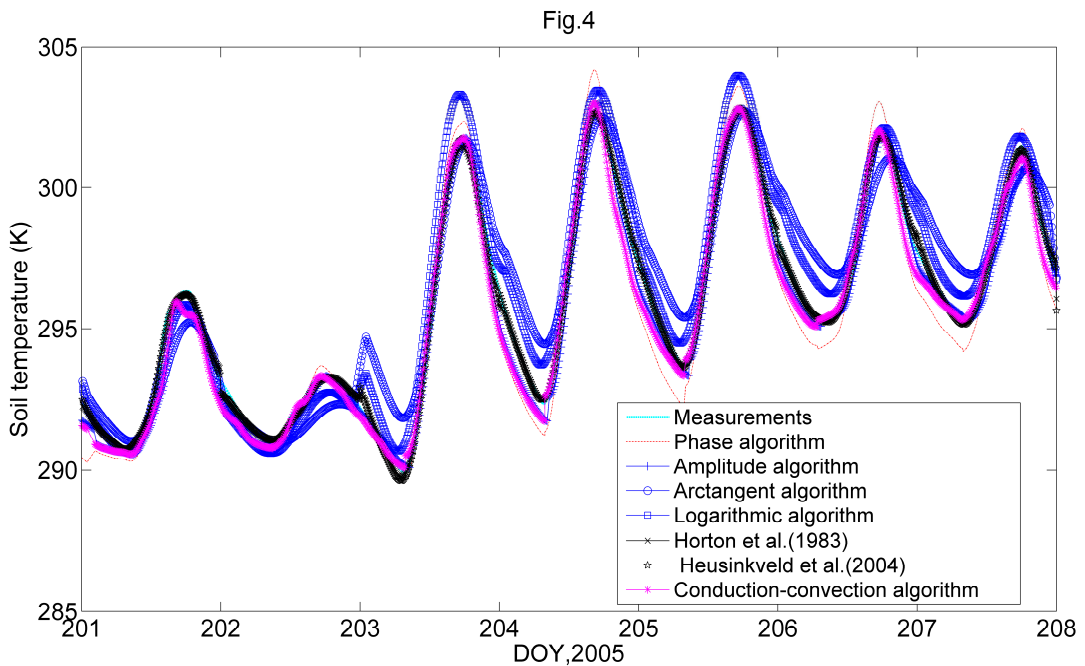


5
 6 Figure 2. Temporal variation of soil apparent thermal diffusivity k ($\text{m}^2 \text{s}^{-1}$) at a bare soil site
 7 over the Loess Plateau from DOY 201 through 207, 2005.



1
 2 Figure 3. Variation of soil apparent thermal diffusivity k ($\text{m}^2 \text{s}^{-1}$) with volumetric soil water
 3 content θ (%) at a bare soil site over the Loess Plateau from DOYs 201 through 207, 2005.

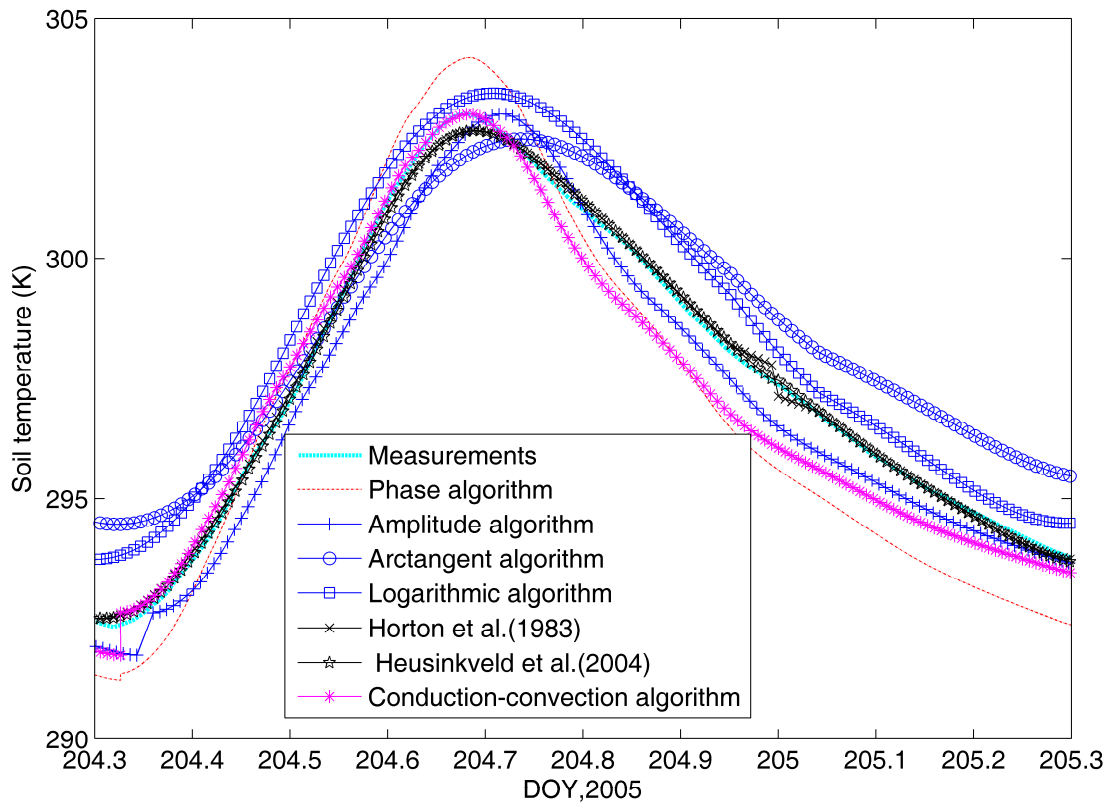
4



5
 6 Figure 4. Comparisons of soil temperature modeled by using Phase algorithm, Amplitude
 7 algorithm, Arctangent algorithm, Logarithmic algorithm, algorithm by Horton et al.(1983),
 8 algorithm by Heusinkveld et al.(2004), and Conduction-convection algorithm, against
 9 measurements of soil temperature at 0.10 m depth at a bare soil site over the Loess Plateau from
 10 DOYs 201 through 207, 2005.

11

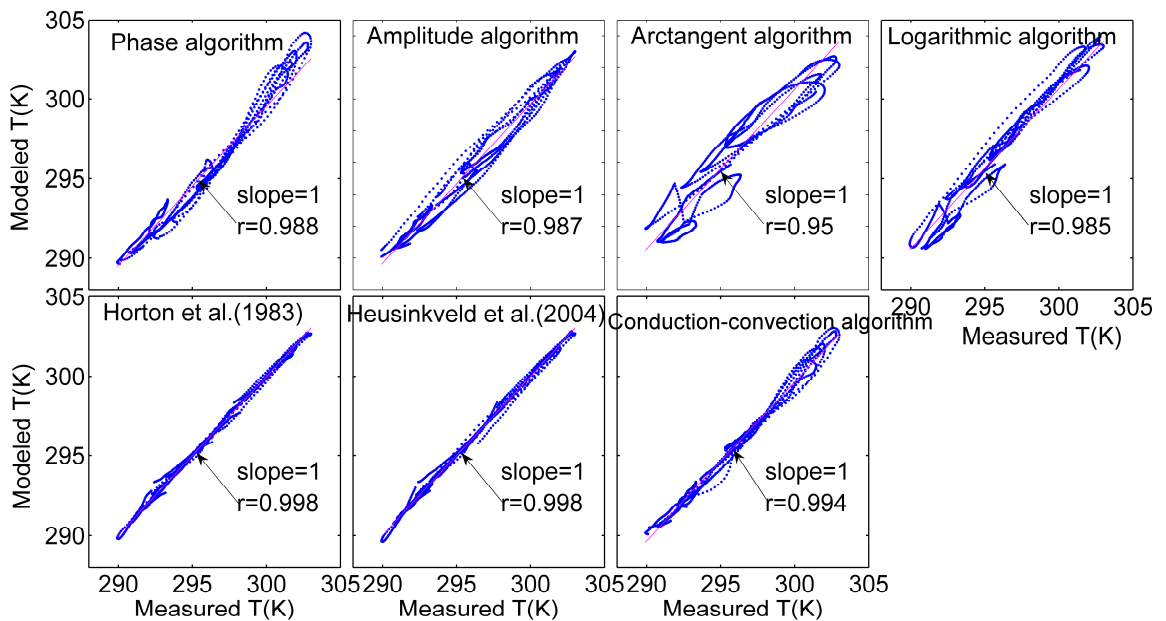
Fig.5



1

2 Figure 5. Comparisons of soil temperature modeled by using Phase algorithm, Amplitude
 3 algorithm, Arctangent algorithm, Logarithmic algorithm, algorithm by Horton et al.(1983),
 4 algorithm by Heusinkveld et al.(2004), and Conduction-convection algorithm, against
 5 measurements of soil temperature at 0.10 m depth at a bare soil site over the Loess Plateau on
 6 DOY 204, 2005.

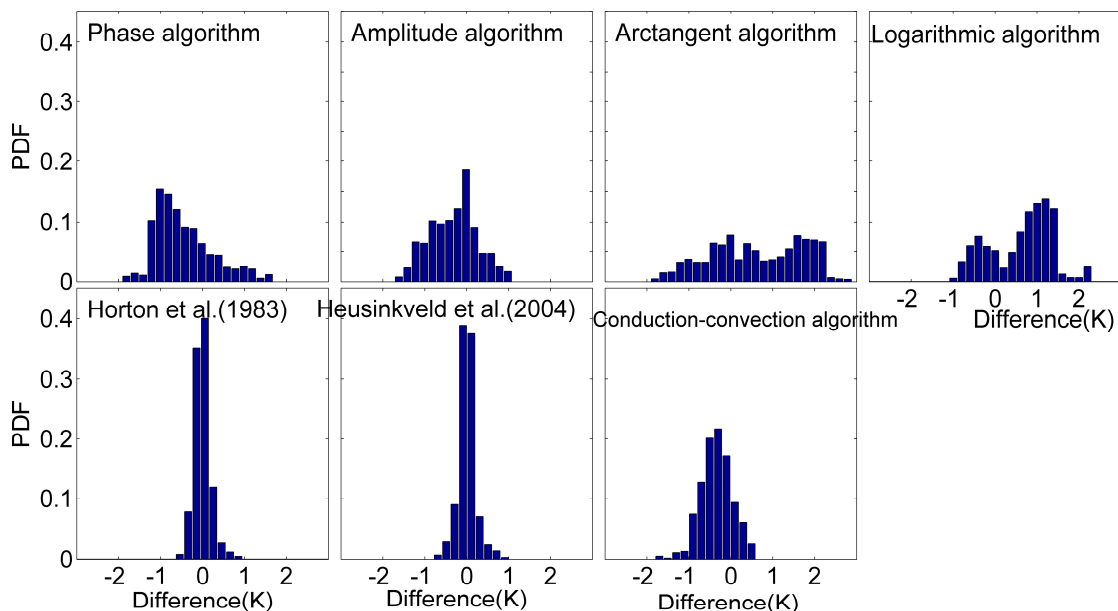
Fig.6



7

1 Figure 6. Scatter plots of the temperature modeled by using Phase algorithm, Amplitude
 2 algorithm, Arctangent algorithm, Logarithmic algorithm, Horton et al.(1983), Heusinkveld et
 3 al.(2004), and Conduction-convection algorithm for the soil depth of 0.10 m against the soil
 4 temperature at 0.10 m depth from DOY 201 to DOY 207, 2005.

Fig.7



5
 6 Figure 7. Empirical probability distribution function, PDF, of subtraction between the temperature
 7 modeled by using the Phase algorithm, Amplitude algorithm, Arctangent algorithm,
 8 Logarithmic algorithm, Horton et al.(1983), Heusinkveld et al.(2004), and Conduction-convection
 9 algorithm for the soil layer ranging from 0.05 m to 0.10 m with the soil temperature at 0.10 m
 10 depth from DOY 201 to DOY 207, 2005.

11

12 Tables

13 Table 1. See another independent file named as “Table 1.doc”

14 Table 2 The maximums, minimums and mean values of k calculated by six algorithms for the
 15 layer of 0.05-0.10m on the Loess Plateau from DOY 201 to DOY 207, 2005.

Name	Max ($k \times 10^7$)	Min ($k \times 10^7$)	Mean ($k \times 10^7$)
Phase algorithm	5.47	2.45	4.24
Amplitude algorithm	2.65	1.69	2.06
Arctangent algorithm	1.60	0.60	1.07
Logarithmic algorithm	3.93	1.50	2.34
HM(Horton et al.,1983)	3.02	1.42	2.22

HM(Heusinkveld et al., 2004)	2.73	1.66	2.30
Conduction-convection algorithm	4.65	2.43	3.92

1

2 Table 3 The values of W calculated by Conduction-convection algorithm for the layer of
3 0.05-0.10m on the Loess Plateau from DOY 201 to DOY 207, 2005.

DOY	$W (\times 10^7 \text{ m s}^{-1})$
201	0.722
202	2.755
203	1.454
204	3.112
205	2.453
206	3.669
207	4.696

4

5 Table 4 The values of the phase shift and the logarithm of amplitude ratio of soil temperature
6 obtained by using one sine function approximation algorithm at the 0.05m and 0.10m depths on
7 the Loess Plateau from DOY 201 to DOY 207, 2005.

DOY	$\Phi_1 - \Phi_2$	$\ln(A_1/A_2)$
201	0.6008	0.6875
202	0.4788	0.7001
203	0.4819	0.5858
204	0.4367	0.6468
205	0.4587	0.6316
206	0.4367	0.7008
207	0.4078	0.7323

8

9 Table 5 Computed Standard Error of the Estimate (SEE) and Normalized Standard Error of the
10 Estimate (NSEE) of soil temperature at 0.10m depth on the Loess Plateau from DOY 201 to DOY
11 207, 2005.

Name	SEE	NSEE
Phase algorithm	0.8288	0.0028
Amplitude algorithm	0.6481	0.0022
Arctangent algorithm	1.2693	0.0043

Logarithmic algorithm	0.9796	0.0033
HM(Horton et al., 1983)	0.1963	0.0006
HM(Heusinkveld et al., 2004)	0.2132	0.0007
Conduction-convection algorithm	0.5091	0.0017

1